Trans. of the Society of Instrument and Control Engineers
Vol.E-4, No.1, 79/88 (2005)

Dead Time Measurement of Stable System by Wavelet under Closed Loop Configuration

Tetsuya TABARU* and Seiichi SHIN**

This paper shows that the wavelet based dead time measurement method, which has been already studied for open loop systems, is also applicable to closed loop systems. The method measures a dead time of an LTI system from a wavelet transform of a cross correlation function between its input and output. At first, we derive the cross correlation function and its cross spectrum for the closed loop case. Next, its wavelet transform is analyzed under certain conditions by using the relation among a wavelet transform of a correlation function and the corresponding spectrum, which we have been already studied. The analysis shows that the dead time is also measurable for the closed loop case although the cross correlation function, the cross spectrum and the wavelet transform have more complicated forms than the open loop case.

Key Words: wavelet transform, correlation analysis, dead time, closed loop system

1. Introduction

We have proposed dead time (pure time delay, transport delay) measurement methods by wavelet transform [1),2)]. The methods measure the dead time from a continuous wavelet transform of a cross correlation function between an input and an output or a step response as follows:

(1) Calculate the wavelet transform of the cross correlation function or the step response by using a complex analyzing wavelet.

(2) Plot phase (argument) contour lines for the wavelet transform (**Fig. 1**). Horizontal axis is assigned for location parameter (time) and vertical for dilation parameter (reciprocal of frequency).

(3) Then the contour lines concentrate at the dead time to be measured as the dilation parameter tends to zero.

Our methods have some advantages over conventional methods. They are applicable even if a degree and a relative degree of a system are unknown. This is common to both the step response based method [1)] and the correlation based method [2)]. The latter method has additional advantages. A limitation on a test input signal is relatively small. The test signal is only required to have a continuous spectrum in a certain frequency range. This is a difference from conventional correlation based methods, which often need special test signals like white noise. In addition, it is robust to disturbances if they have no correlation with inputs. The method was applied to real system: an air conditioner system [4)] and a boiler plant [5),6)]. The results indicated efficiency of our method.

The preceding studies [2),3)] have provided the reason why the method can measure a dead time of a system when it is an open loop, LTI (linear time invariant) and SISO (single-input single-output) system. However, no analysis has been given for the case of a closed loop system regardless of its importance. There are many systems operated under closed loop conditions. For some of them, a feedback control is necessary for stability. It means that our preceding theory can't cover such a case. In spite of this, several applications of our method were carried out for closed loop systems. Nakano *et al.* succeeded in the dead time estimation of the boiler plant under feedback control [5),6)]. From the above background, we should analyze the method under closed loop settings and investigate its limitations. This is important when applying the method to wide range of real systems.

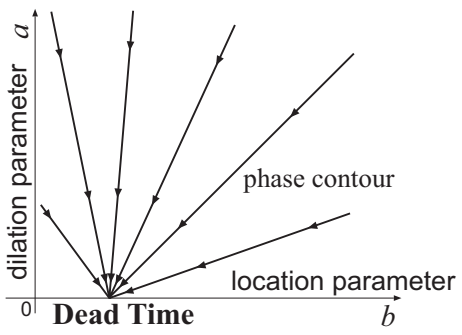

Fig. 1 The dead time measuring method from a phase contour plot of wavelet transform.

* Research & Development Headquarters, Yamatake Corporation, 1–12–2 Kawana, Fujisawa, Kanagawa, Japan
** Department of Systems Engineering, the University of Electro-Communications, 1–5–1 Chofu-ga-oka, Chofu, Tokyo, Japan

The objective of this paper is to show that our method is also applicable to closed loop LTI systems under certain conditions. The target is limited to stable SISO systems, so that it is relatively easy to calculate a cross correlation function between an input and an output. The method can be employed for both open and closed loop systems. It follows that we don't need to know whether an object to measure is a part of a closed loop system or not. This is a new advantage of our proposed method.

Section 2 describes our preceding studies related to this paper. Problem settings are given in section 3. Section 4 is devoted to calculate a cross correlation function and cross spectrum density between an input and an output. Since both the correlation function and the spectrum density are too complicated to analyze directly, pre-analyses are provided in section 5. Section 6 gives detailed analyses on phase contour lines to reveal the capability of our method. To achieve it, we will suppose additional conditions so that the analyses are simple and practical. In section 7, numerical simulations show validity of our discussion. Section 8 concludes this paper.

Notation: The set of real numbers will be represented by $\boldsymbol{R}$ and the set of complex numbers by $\boldsymbol{C}$. The asterisk * denotes complex conjugation and $\angle$ denotes a phase (argument) value. The Fourier transform of a time-domain signal $x(t)$ is defined by $X(\omega) = \int_{-\infty}^{+\infty} x(t)e^{-j\omega t}\mathrm{d}t$. In this study, we use this definition to agree with the Laplace transform [1]. The inner product over the space of square integrable functions $L^2(\boldsymbol{R})$ is defined by $\langle x(t), y(t)\rangle = \int_{-\infty}^{+\infty} x^*(t)y(t)\mathrm{d}t$. The cross correlation function between $u(t) \in \boldsymbol{R}$ and $y(t+t') \in \boldsymbol{R}$ is denoted by $\phi_{u(t),y(t+t')}(\tau)$ and its definition is as follows:

$$\phi_{u(t),y(t+t')}(\tau) = \lim_{T\to\infty} \frac{1}{2T}\int_{-T}^{T} u(t)y(t+t'+\tau)\mathrm{d}t.$$

Thus $\Phi_{u(t),y(t+t')}(\omega)$, which is the Fourier transform of $\phi_{u(t),y(t+t')}(\tau)$, is the cross spectrum density between $u(t)$ and $y(t+t')$. If $t'=0$, they are simply denoted by $\phi_{uy}(\tau)$ and $\Phi_{uy}(\omega)$ respectively. Similarly, $\phi_{uu}(\tau)$ is the auto correlation function of $u(t) \in \boldsymbol{R}$ and $\Phi_{uu}(\omega)$ is the power spectrum density.

An analyzing wavelet is denoted by $\psi(t)$. In this paper, $\psi(t)$ is supposed to be a complex function. Wavelet bases are represented by $\psi_{a,b}(t)$ and defined by $\psi_{a,b}(t) = \psi((t-b)/a)/\sqrt{a}$. The parameter a is a dilation parameter (or scaling parameter, scale parameter) and b is a location parameter (or translation parameter, shift parameter). The wavelet transform is defined by using this basis as $\tilde{x}(a,b) = \langle \psi_{a,b}(t), x(t)\rangle$. Note that the parameter a is restricted to be positive real numbers in this paper. The domain of the parameter b is $\boldsymbol{R}$.

(1) There is a slight difference from the definition in the previous paper [7]. It has the additional constant $1/\sqrt{2\pi}$.

2. Preceding Results

This section gives a brief explanation about two preceding results necessary for this paper. The first is a relation between a wavelet transform of a correlation function and the corresponding spectrum density [7] (Section 2. 1). The second is a theoretical study of our method for the open loop case (Section 2. 2).

2. 1 Wavelet Transform of Correlation Function and Spectrum Density

Consider a wavelet transform of a cross correlation function $\phi_{xy}(\tau)$. It is defined by $\tilde{\phi}_{xy}(a,b) = \langle \psi_{a,b}(\tau), \phi_{xy}(\tau)\rangle$. The following lemma is about a relation between the wavelet transform $\tilde{\phi}_{xy}(a,b)$ and the corresponding spectrum density $\Phi_{xy}(\omega)$ [4),7)].

Lemma 1. Assume that $\Phi_{xy}(\omega)$ and $\psi(t)$ are n-times differentiable, and there is a constant C_ϕ satisfying $|\phi_{xy}(\tau)| \le C_\phi/(1+|\tau|)^{n+2}$. Then, for an arbitrary constant ω_0,

$$\tilde{\phi}_{xy}(a,b) = \frac{\psi^*(0)}{\sqrt{a}}\Phi_{x(t),y(t+b)}\Big(\frac{\omega_0}{a}\Big) + \sum_{k=1}^{n-1} Q_k + R_n(1)$$

where

$$Q_k = \frac{\sqrt{a}}{2\pi k!}\Phi^{(k)}_{x(t),y(t+b)}\Big(\frac{\omega_0}{a}\Big)\int_{-\infty}^{+\infty} \lambda^k \Psi^*(\omega_0 + a\lambda)\mathrm{d}\lambda$$

In addition, $|R_n|$ is bounded as follows.

$$|R_n| \le \frac{\sqrt{a}}{n!}\max_{\omega}\Big|\Phi^{(n)}_{x(t),y(t+b)}(\omega)\Big|\int_{-\infty}^{+\infty}|\lambda^n\Psi^*(\omega_0+a\lambda)|\mathrm{d}\lambda$$

Proof: See the preceding paper [7]. The conditions on $\psi(t)$ and $\phi(\tau)$ are needed to ensure the boundedness of $|R_n|$. ∎

The above lemma implies

$$\frac{\sqrt{a}}{\psi^*(0)}\tilde{\phi}_{xy}(a,b) \approx \Phi_{x(t),y(t+b)}\Big(\frac{\omega_0}{a}\Big) \qquad (2)$$

if Q_k and R_n are sufficiently small. This equation allows us to consider a wavelet transform of a correlation function as an estimate of the corresponding spectrum density. In order to relate the wavelet transform with the spectrum density, we have to select an appropriate analyzing wavelet such that Q_k becomes small. An example of such a wavelet is a function that can be expressed as a product of an even window function and a complex sinusoid $e^{j\omega_p t}$, that is

$$\psi(t) = w(t)e^{j\omega_p t}, \quad w(t) = w(-t) \in \boldsymbol{R} \tag{3}$$

where ω_p is the center frequency, and $w(t)$ is a window function. In the rest of this paper, we assume use of analyzing wavelets such that the approximation (2) holds, and denote the center frequency of such a wavelet by ω_p.

2.2 Dead Time Measurement for Open Loop Systems

We provide give a mathematical interpretation of our proposed method for stable open loop systems. The explanation is based on our past paper [3] and the result of the section 2.1. We also note that the same result can be derived from a self-similarity property of an impulse response around a dead time [2].

The open loop system treated in our studies is a SISO (single-input single-output) LTI (linear time-invariant) system whose transfer function is $G(s) = G_R(s)e^{-Ls}$, where $G_R(s)$ is a strictly proper rational transfer function with real coefficients and L is a dead time of the system. An input and an output of the system are denoted by $u(t)$ and $y(t)$ respectively.

From $\Phi_{u(t),y(t+b)}(\omega) = G_R(j\omega)\, e^{-j\omega L}\, \Phi_{uu}(\omega)\, e^{j\omega b}$ and the equation (2), it can be derived that $\angle\tilde{\phi}_{uy}(a,b) = \angle G_R(j\omega_p/a) + (b-L)\omega_p/a - \angle\psi(0)$. This equation can be rewritten as

$$b = \frac{\angle G_R(j\omega_p/a) - \angle\tilde{\phi}_{uy}(a,b) - \angle\psi(0)}{\omega_p}\, a + L. \tag{4}$$

On a phase contour line of $\tilde{\phi}_{uy}(a,b)$, $\angle\tilde{\phi}_{uy}(a,b)$ takes the same value. For smaller a (*i.e.* higher frequency), $\angle G_R(j\omega_p/a)$ is almost constant because $G_R(j\omega)$ becomes steady value when ω is higher than a certain frequency. Consequently, the phase contour lines are expressed by the following equation.

$$b = sa + L, \quad s \in \boldsymbol{R} \tag{5}$$

It implies that any contour line concentrates at $b = L$, where the dead time is located, as $a \to 0$.

3. Problem Settings

This section describes a closed loop system considered in this paper.

Figure 2 illustrates a block diagram of the closed loop system. It consists of a controller C and a controlled object P, which has a dead time element to be measured at its input. Both of them are linear and time-invariant. In addition, we assume that C is proper and $G_R(s)$ is strictly proper. An input and an output of the overall system are $r(t) \in \boldsymbol{R}$ and $y(t) \in \boldsymbol{R}$ respectively. An output of the controller is $u(t) \in \boldsymbol{R}$, which is connected to an input of the controlled object. A disturbance $v(t) \in \boldsymbol{R}$ is added to the output of P. Assume that P and the overall system are stable and $v(t)$ has no correlation with $r(t)$ (*i.e.* $\phi_{rv}(\tau) = \Phi_{rv}(\omega) = 0$).

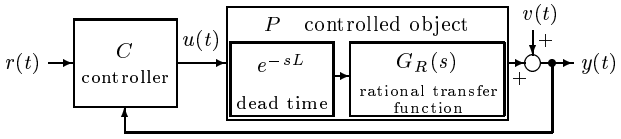

Fig. 2 Closed loop system considered in this paper.

The state variable equations of the controlled object are as follows

$$\dot{\boldsymbol{x}}_p(t) = A_p\boldsymbol{x}_p(t) + \boldsymbol{b}_p u(t-L) \tag{6-a}$$
$$y(t) = \boldsymbol{c}_p^T\boldsymbol{x}_p(t) + v(t) \tag{6-b}$$

where $\boldsymbol{x}_p(t)$ is its state vector. This system is assumed to be controllable and observable. The state variable equations of the controller are

$$\dot{\boldsymbol{x}}_c(t) = A_c\boldsymbol{x}_c(t) + [\,\boldsymbol{b}_{c1}\ \boldsymbol{b}_{c2}\,]\,\boldsymbol{f}_{rv}(t) \tag{7-a}$$
$$u(t) = \boldsymbol{c}_c^T\boldsymbol{x}_c(t) + [\,d_{c1}\ d_{c2}\,]\,\boldsymbol{f}_{rv}(t) \tag{7-b}$$

where $\boldsymbol{f}_{rv}(t) = [\,r(t)\ v(t)\,]^T$ and $\boldsymbol{x}_c(t)$ is controller's state vector. Now, define $\boldsymbol{x}(t) = [\,\boldsymbol{x}_p(t)\ \boldsymbol{x}_c(t)\,]^T$. Therefore, the overall state variable equations are the following.

$$\dot{\boldsymbol{x}}(t) = A_1\boldsymbol{x}(t) + A_2\boldsymbol{x}(t-L) + B_1\,\boldsymbol{f}_{rv}(t) + B_2\,\boldsymbol{f}_{rv}(t-L) \tag{8-a}$$
$$u(t) = C_u\boldsymbol{x}(t) + D_u\,\boldsymbol{f}_{rv}(t) \tag{8-b}$$
$$y(t) = C_y\boldsymbol{x}(t) + v(t) \tag{8-c}$$

where

$$A_1 = \begin{bmatrix} A_p & 0 \\ \boldsymbol{b}_{c2}\boldsymbol{c}_p^T & A_c \end{bmatrix},\ A_2 = \begin{bmatrix} \boldsymbol{b}_p d_{c2}\boldsymbol{c}_p^T & \boldsymbol{b}_p\boldsymbol{c}_c^T \\ 0 & 0 \end{bmatrix} \tag{9-a}$$

$$B_1 = \begin{bmatrix} 0 & 0 \\ \boldsymbol{b}_{c1} & \boldsymbol{b}_{c2} \end{bmatrix},\ B_2 = \begin{bmatrix} \boldsymbol{b}_p d_{c1} & \boldsymbol{b}_p d_{c2} \\ 0 & 0 \end{bmatrix} \tag{9-b}$$

$$C_u = [\,d_{c2}\boldsymbol{c}_p^T\ \boldsymbol{c}_c^T\,],\ C_y = [\,\boldsymbol{c}_p^T\ 0\,] \tag{9-c}$$

$$D_u = [\,d_{c1}\ d_{c2}\,]. \tag{9-d}$$

This is one of the simplest retarded systems [8]. Without loss of generality, we assume $\boldsymbol{x}(t) = \boldsymbol{f}_{rv}(t) = 0$ for $t < 0$ because the initial response doesn't affect correlation functions for stable systems.

This closed loop system involves various configurations of a feedback controller for a SISO system. For example, rational transfer function controllers, two degrees of freedom controllers, and PID controllers.

Remark: More precisely, if a PID controller has a "ideal" derivative term, the controller is not included in the problem settings. However, it doesn't matter in actual control. ∎

The measurement procedure is the same as the open loop case. In the above settings, an exogenous input is added to $r(t)$ (input of the overall system) instead of $u(t)$ (input of the controlled object), but this is not a fundamental difference. In fact, setting $d_{c1} = 1$ allows us to add the exogenous signal to $u(t)$ directly.

4. Derivation of Cross Correlation Function and Cross Spectrum Density

The aim of this section is to represent the cross correlation function between $u(t)$ and $y(t)$ by using the auto correlation functions of $r(t)$ and $y(t)$. Similarly, the corresponding spectrum density is also derived. They are necessary for later analyses. First, we calculate $\phi_{uy}(\tau)$ (section 4. 1), and then obtain $\Phi_{uy}(\omega)$ (section 4. 2). The proofs of the lemma 2, 3 and 4 are straightforward calculations. Thus we only show brief outlines for them.

4. 1 Cross Correlation Function

At first, consider the response of the state variable for the system (8). The system is a simple retarded system and its state variable equation can be written as

$$\dot{\boldsymbol{x}}(t) = A_1\boldsymbol{x}(t) + A_2\boldsymbol{x}(t-L) + \boldsymbol{f}(t), \tag{10}$$

where $\boldsymbol{f}(t) = B_1\boldsymbol{f}_{rv}(t) + B_2\boldsymbol{f}_{rv}(t-L)$. The response is given by the following lemma.

Lemma 2. If $\boldsymbol{x}(t) = 0$ and $\boldsymbol{f}(t) = 0$ for $t < 0$, the response of the system (10) is

$$\boldsymbol{x}(t) = \sum_{k=0}^{\infty}\int_0^t g_k(t-\xi)\boldsymbol{f}(\xi - kL)\mathrm{d}\xi, \tag{11}$$

where $g_k(t)$ is defined recursively as follows.

$$g_k(t) = \begin{cases} e^{A_1 t}, \ k = 0, \ t \geq 0 \\ \int_0^t e^{A_1(t-\xi)} A_2\, g_{k-1}(\xi)\mathrm{d}\xi, \ k \geq 1, \ t \geq 0 \\ 0, \ t < 0 \end{cases} \tag{12}$$

Proof: For $t \geq 0$, the response of the system (10) is[8)]

$$\boldsymbol{x}(t) = \int_0^t e^{A_1(t-\xi)}(\boldsymbol{f}(\xi) + A_2\boldsymbol{x}(\xi - L))\mathrm{d}\xi.$$

The result is obtained by applying this equation recursively. ∎

The next lemma enables us to represent $u(t)$ and $y(t)$ of the system (8) by $r(t)$ and $v(t)$.

Lemma 3. Consider the system (8). If $\boldsymbol{x}(t) = \boldsymbol{f}_{rv}(t) = 0$ for $t < 0$, $u(t)$ and $y(t)$ are

$$u(t) = \sum_{k=0}^{\infty} g_{u,k}(t)\boldsymbol{f}_{rv}(\xi - kL)\mathrm{d}\xi + D_u\,\boldsymbol{f}_{rv}(t) \tag{13-a}$$

$$y(t) = \sum_{k=1}^{\infty} g_{y,k}(t)\boldsymbol{f}_{rv}(\xi - kL)\mathrm{d}\xi + v(t), \tag{13-b}$$

where $g_{u,k}(t)$ and $g_{y,k}(t)$ are defined by

$$g_{u,k}(t) = [\, g_{ur,k}(t)\ g_{uv,k}(t)\,] = \begin{cases} C_u\, g_k(t)B_1 & k = 0 \\ C_u(g_k(t)B_1 + g_{k-1}(t)B_2) & k \geq 1 \end{cases} \tag{14-a}$$

$$g_{y,k}(t) = [\, g_{yr,k}(t)\ g_{yv,k}(t)\,] = C_y(g_k(t)B_1 + g_{k-1}(t)B_2). \tag{14-b}$$

Proof: The response of (8-a) is the sum of responses of the following two retarded systems.

$$\dot{\boldsymbol{x}}(t) = A_1\boldsymbol{x}(t) + A_2\boldsymbol{x}(t-L) + B_1\boldsymbol{f}_{rv}(t) \tag{15-a}$$

$$\dot{\boldsymbol{x}}(t) = A_1\boldsymbol{x}(t) + A_2\boldsymbol{x}(t-L) + B_2\boldsymbol{f}_{rv}(t-L) \tag{15-b}$$

From lemma 2, the responses of the above systems are

$$\boldsymbol{x}(t) = \sum_{k=0}^{\infty}\int_0^t g_k(t-\xi)B_1\boldsymbol{f}_{rv}(\xi - kL)\mathrm{d}\xi \tag{16-a}$$

$$\boldsymbol{x}(t) = \sum_{k=1}^{\infty}\int_0^t g_{k-1}(t-\xi)B_2\boldsymbol{f}_{rv}(\xi - kL)\mathrm{d}\xi \tag{16-b}$$

and their sum is the response of the system (8-a). The results are obtained by substituting the response into the equation (8-b) and (8-c). ∎

Now, we can derive a lemma about the cross correlation function $\phi_{uy}(\tau)$.

Lemma 4. Let $\phi_{rr,vv}(\tau) = [\,\phi_{rr}(\tau)\ \phi_{vv}(\tau)\,]^T$. Then

$$\begin{aligned}\phi_{uy}(\tau) = &\sum_{k=-\infty}^{+\infty}\int_{-\infty}^{+\infty}\boldsymbol{h}_k^T(\tau - t)\phi_{rr,vv}(t - kL)\mathrm{d}t \\ &+ \sum_{k=-\infty}^{0}\int_{-\infty}^{+\infty} g_{uv,-k}(t-\tau)\phi_{vv}(t - kL)\mathrm{d}t \\ &+ d_{c2}\phi_{vv}(\tau).\end{aligned} \tag{17}$$

where $\boldsymbol{h}_k(t) = [\, h_{r,k}(t)\ h_{v,k}(t)\,]^T$ and $h_{r,k}(t)$ and $h_{v,k}(t)$ are defined as follows.

$$h_{r,k}(t) = \begin{cases} \displaystyle\sum_{l=1-k}^{+\infty}\int_0^{\infty} g_{ur,l}(\xi - t)g_{yr,k+l}(\xi)\mathrm{d}\xi, & k \leq 0 \\ \displaystyle d_{c1}g_{yr,k}(t) + \sum_{l=0}^{+\infty}\int_0^{\infty} g_{ur,l}(\xi - t)g_{yr,k+l}(\xi)\mathrm{d}\xi, & k \geq 1 \end{cases}$$

$$h_{v,k}(t) = \begin{cases} \displaystyle\sum_{l=1-k}^{+\infty}\int_0^{\infty} g_{uv,l}(\xi - t)g_{yv,k+l}(\xi)\mathrm{d}\xi, & k \leq 0 \\ \displaystyle d_{c2}g_{yv,k}(t) + \sum_{l=0}^{+\infty}\int_0^{\infty} g_{uv,l}(\xi - t)g_{yv,k+l}(\xi)\mathrm{d}\xi, & k \geq 1 \end{cases}$$

Proof: Let $z_i(t) = \int_{-\infty}^{+\infty} q_i(t-\xi) f_i(\xi - k_i L)\mathrm{d}\xi$ for $i = 1, 2$. Suppose that $\int_{-\infty}^{+\infty} |q_i(t)|\mathrm{d}t$ is bounded for each i. Then

$$\phi_{z_1 z_2}(\tau) = \int_{-\infty}^{+\infty} h(\tau - t)\phi_{f_1 f_2}(t - (k_1 - k_2)L)\mathrm{d}t.$$

where $h(t) = \int_0^t q_1(\xi - t) q_2(\xi)\mathrm{d}\xi$. We can reach the result by using the relation and $\phi_{rv}(\tau) = 0$. The assumptions on stability of P and the overall system assure the boundedness of $\boldsymbol{h}_k(t)$. The rest of the proof is similar to the proof of lemma 6 though the calculation is performed in frequency domain. Thus, the details are omitted. ∎

4.2 Cross Spectrum Density

The calculation of the cross spectrum density takes has steps. In the first step, $U(\omega)$ and $Y(\omega)$ are expressed by $R(\omega)$ and $V(\omega)$ (lemma 5). This part uses the results of the lemmas 2 and 3. The cross spectrum density between $u(t)$ and $y(t)$ is derived in the second step (lemma 6).

Before the lemma 5, let us introduce $G_R(s)$, $G_C(s)$, $G_{C1}(s)$, $G_{C2}(s)$, and $G_{LP}(s)$ as below:

$$G_R(s) = \boldsymbol{c}_p^T (sI - A_p)^{-1} \boldsymbol{b}_p \tag{18}$$

$$\begin{aligned} G_C(s) &= [\, G_{C1}(s)\ G_{C2}(s)\,] \\ &= \boldsymbol{c}_c^T (sI - A_c)^{-1} [\, \boldsymbol{b}_{c1}\ \boldsymbol{b}_{c2}\,] + [\, d_{c1}\ d_{c2}\,] \end{aligned} \tag{19}$$

$$G_{LP}(s) = G_{C2}(s) G_R(s). \tag{20}$$

Each transfer function can be interpreted as follows: $G_R(s)$ is the rational transfer function in the controlled object, $G_{C1}(s)$ is the transfer function of the controller C from $r(t)$ to $u(t)$, $G_{C2}(s)$ is similar but from $v(t)$, and $G_{LP}(s)$ is the open-loop transfer function without the dead time element.

Lemma 5. For the system (8),

$$U(\omega) = \sum_{k=0}^{\infty} e^{-j\omega k L} G_{u,k}(j\omega) \boldsymbol{F}_{rv}(\omega) + D_u \boldsymbol{F}_{rv}(\omega) \tag{21-a}$$

$$Y(\omega) = \sum_{k=1}^{\infty} e^{-j\omega k L} G_{y,k}(j\omega) \boldsymbol{F}_{rv}(\omega) + V(\omega) \tag{21-b}$$

where $G_{u,k}(j\omega)$ and $G_{y,k}(j\omega)$ are the Fourier transforms of $g_{u,k}(t)$ and $g_{y,k}(t)$, and $\boldsymbol{F}_{rv}(\omega) = [R(\omega)\ V(\omega)]^T$ is the Fourier transform of $\boldsymbol{f}_{rv}(t)$. In addition, for ω such that $|G_{LP}(j\omega)| < 1$, $G_{u,k}(j\omega)$ and $G_{y,k}(j\omega)$ can be represented as follows:

$$G_{u,k}(j\omega) = \begin{cases} G_C(j\omega) - D_u, & k = 0 \\ (G_{LP}(j\omega))^k G_C(j\omega), & k \geq 1 \end{cases} \tag{22-a}$$

$$G_{y,k}(j\omega) = G_R(j\omega)(G_{LP}(j\omega))^{k-1} G_C(j\omega). \tag{22-b}$$

Proof: The former part of the lemma (the equation (21)) is obvious from the equation (13), so we will only prove the latter.

Now define $\boldsymbol{b}_{p0} \in \boldsymbol{R}^4$ by $\boldsymbol{b}_{p0} = [\, \boldsymbol{b}_p^T\ \boldsymbol{0}^T\,]^T$. Applying the Laplace transform to the lemma 2 and using $A_2 = \boldsymbol{b}_{p0} C_u$, we obtain $G_{k+1}(s) = G_0(s) A_2 G_k = G_0(s)\, \boldsymbol{b}_{p0} C_u G_k(s)$. From a property of the inverse of block triangular matrices, $G_0(s)$ can be expressed as follows.

$$G_0(s) = \begin{bmatrix} (sI - A_p)^{-1} & 0 \\ (sI - A_c)^{-1} \boldsymbol{b}_{c2} \boldsymbol{c}_p^T (sI - A_p)^{-1} & (sI - A_c)^{-1} \end{bmatrix}$$

It follows that $G_R(s) = C_y G_0(s) \boldsymbol{b}_{p0}$, $G_C(s) = D_u + C_u G_0(s) B_1$, and $G_{LP}(s) = C_u G_0(s) \boldsymbol{b}_{p0}$. Therefore

$$C_u G_0(s) B_1 = G_C(s) - D_u \tag{23}$$

$$C_u G_{k+1}(s) = G_{LP}(s) C_u G_k(s) \tag{24}$$

$$C_y G_{k+1}(s) = G_R(s) C_u G_k(s) \tag{25}$$

for $k \geq 0$. Now, we rewrite the equation (14) by applying the Laplace transform.

$$\begin{aligned} G_{u,k}(s) &= [\, G_{ur,k}(s)\ \ G_{uv,k}(s)\,] \\ &= \begin{cases} C_u G_0(s) B_1, & k = 0 \\ C_u (G_k(s) B_1 + G_{k-1}(s) B_2), & k \geq 1 \end{cases} \\ G_{y,k}(s) &= [\, G_{yr,k}(s)\ \ G_{yv,k}(s)\,] \\ &= C_y (G_k(s) B_1 + G_{k-1}(s) B_2) \end{aligned}$$

The equation (22) is obtained by substituting the equations (23), (24), (25) and $B_2 = \boldsymbol{b}_{p0} D_u$ into the above equations. Note that the summation of the equation (21) has finite values only for ω satisfying $|G_{LP}(j\omega)| < 1$. ∎

The next step is a calculation of $\Phi_{uy}(\omega)$.

Lemma 6. For ω such that $|G_{LP}(j\omega)| < 1$,

$$\begin{aligned} \Phi_{uy}(\omega) = &\sum_{k=-\infty}^{+\infty} \boldsymbol{H}_k(j\omega) \boldsymbol{\Phi}_{rr,vv}(\omega) e^{-j\omega k L} \\ &+ \sum_{k=-\infty}^{0} (G_{LP}^*(j\omega))^{-k} G_{C2}^*(j\omega) \Phi_{vv}(\omega) e^{-j\omega k L} \end{aligned} \tag{26}$$

where $\boldsymbol{\Phi}_{rr,vv}(\omega) = [\Phi_{rr}(\omega)\ \Phi_{vv}(\omega)]^T$ and

$$\boldsymbol{H}_k(j\omega) = \begin{cases} \dfrac{G_R(j\omega)}{1 - |G_{LP}(j\omega)|^2} [\, |G_{C1}(j\omega)|^2\ |G_{C2}(j\omega)|^2\,], & k = 1 \\ (G_{LP}^*(j\omega))^{1-k} \boldsymbol{H}_1(j\omega), & k < 1 \\ (G_{LP}(j\omega))^{k-1} \boldsymbol{H}_1(j\omega), & k > 1. \end{cases} \tag{27}$$

Proof: From $\Phi_{rv} = 0$ (the assumption that $v(t)$ has no correlation with $r(t)$),

$$\begin{aligned} &G_{u,k'}^* \boldsymbol{F}_{rv}^* G_{y,k''} \boldsymbol{F}_{rv} \\ &= (G_{ur,k'} R + G_{uv,k'} V)^* (G_{yr,k''} R + G_{yv,k''} V) \\ &= G_{ur,k'}^* G_{yr,k''} \Phi_{rr} + G_{uv,k'}^* G_{yv,k''} \Phi_{vv} \end{aligned}$$

(ω is omitted for simplicity). By using the relation and the lemma 5, we can represent $\Phi_{uy}(\omega)$ as follows:

$$\begin{aligned}\Phi_{uy}(\omega) &= U^*(\omega)Y(\omega)\\ &= \sum_{k'=0}^{\infty}\sum_{k''=1}^{\infty} G^*_{ur,k'}(j\omega)G_{yr,k''}(j\omega)\Phi_{rr}(\omega)e^{j\omega(k'-k'')L}\\ &+ \sum_{k'=0}^{\infty}\sum_{k''=1}^{\infty} G^*_{uv,k'}(j\omega)G_{yv,k''}(j\omega)\Phi_{vv}(\omega)e^{j\omega(k'-k'')L}\\ &+ d_{c1}\sum_{k''=1}^{\infty} G_{yr,k''}(j\omega)\Phi_{rr}(\omega)e^{-j\omega k''L}\\ &+ d_{c2}\sum_{k''=1}^{\infty} G_{yv,k''}(j\omega)\Phi_{vv}(\omega)e^{-j\omega k''L}\\ &+ \sum_{k'=0}^{\infty} G^*_{uv,k'}(j\omega)\Phi_{vv}(\omega)e^{j\omega k'L} + d_{c2}\Phi_{vv}(\omega).\end{aligned}$$

Let $k = k'' - k'$. Then the first term of the equation becomes

$$\begin{aligned}&\sum_{k'=0}^{\infty}\sum_{k=1-k'}^{\infty} G^*_{ur,k'}(j\omega)G_{yr,k+k'}(j\omega)\Phi_{rr}(\omega)e^{-j\omega kL}\\ &= \sum_{k=-\infty}^{\infty}\sum_{\substack{k'=0\\ k+k'\geq 1}}^{\infty} G^*_{ur,k'}(j\omega)G_{yr,k+k'}(j\omega)\Phi_{rr}(\omega)e^{-j\omega kL}.\end{aligned}$$

The same holds for the second term. For integers k and k', it is easy to confirm the following facts.

- For $k > 0$: $k' \geq 0$ and $k + k' \geq 1 \Rightarrow k' \geq 0$.
- For $k \leq 0$: $k' \geq 0$ and $k + k' \geq 1 \Rightarrow k' \geq 1 - k$

Thus, the previous representation of $\Phi_{uy}(\omega)$ can be rewritten as

$$\begin{aligned}\Phi_{uy}(\omega) &= d_{c1}\sum_{k=1}^{+\infty} G_{yr,k}(j\omega)\Phi_{rr}(\omega)e^{-j\omega kL}\\ &+ \sum_{k=1}^{+\infty}\sum_{k'=0}^{+\infty} G^*_{ur,k'}(j\omega)G_{yr,k+k'}(j\omega)\Phi_{rr}(\omega)e^{-j\omega kL}\\ &+ \sum_{k=-\infty}^{0}\sum_{k'=1-k}^{\infty} G^*_{ur,k'}(j\omega)G_{yr,k+k'}(j\omega)\Phi_{rr}(\omega)e^{-j\omega kL}\\ &+ d_{c2}\sum_{k=1}^{+\infty} G_{yv,k}(j\omega)\Phi_{vv}(\omega)e^{-j\omega kL}\\ &+ \sum_{k=1}^{+\infty}\sum_{k'=0}^{+\infty} G^*_{uv,k'}(j\omega)G_{yv,k+k'}(j\omega)\Phi_{vv}(\omega)e^{-j\omega kL}\\ &+ \sum_{k=-\infty}^{0}\sum_{k'=1-k}^{+\infty} G^*_{ur,k'}(j\omega)G_{yr,k+k'}(j\omega)\Phi_{rr}(\omega)e^{-j\omega kL}\\ &+ \sum_{k'=-\infty}^{0} G^*_{uv,-k'}(j\omega)\Phi_{vv}(\omega)e^{j\omega k'L} + d_{c2}\Phi_{vv}(\omega).\end{aligned}$$

Now, let $\boldsymbol{H}_k(j\omega) = [H_{r,k}(j\omega)\ H_{v,k}(j\omega)]^T$ and

$$H_{r,k}(j\omega) = \begin{cases}\displaystyle\sum_{k'=0}^{\infty} G^*_{ur,k'}(j\omega)G_{yr,k+k'}(j\omega)\\ \qquad + d_{c1}G_{yr,k}(j\omega), & k \geq 1\\ \displaystyle\sum_{k'=1-k}^{\infty} G^*_{ur,k'}(j\omega)G_{yr,k+k'}(j\omega), & k \leq 0\end{cases}$$

$$H_{v,k}(j\omega) = \begin{cases}\displaystyle\sum_{k'=0}^{\infty} G^*_{uv,k'}(j\omega)G_{yv,k+k'}(j\omega)\\ \qquad + d_{c2}G_{yv,k}(j\omega), & k \geq 1\\ \displaystyle\sum_{k'=1-k}^{\infty} G^*_{uv,k'}(j\omega)G_{yv,k+k'}(j\omega), & k \leq 0.\end{cases}$$

Then the equation (26) is obtained by substituing the equation (22-a) into $G^*_{uv,-k}(j\omega)$.

The equation (27) can be proven by the following way. From the equation (22), for $k \geq 1$, $G_{ur,0}(j\omega) = G_{C1}(j\omega) - d_{c1}$, $G_{ur,k}(j\omega) = (G_{LP}(j\omega))^k G_{C1}(j\omega)$, and $G_{yr,k}(j\omega) = G_R(j\omega)(G_{LP}(j\omega))^{k-1}G_{C1}(j\omega)$. By substituting them into $H_{r,k}(j\omega)$, we can rewritten it as

$$G_R(j\omega)|G_{C1}(j\omega)|^2(G_{LP}(j\omega))^{k-1}\sum_{k'=0}^{\infty}|G_{LP}(j\omega)|^{2k'}.$$

If $|G_{LP}(j\omega)| < 1$, the summation is finite and

$$H_{r,k}(j\omega) = \frac{G_R(j\omega)|G_{C1}(j\omega)|^2(G_{LP}(j\omega))^{k-1}}{1 - |G_{LP}(j\omega)|^2}.$$

Also for $k \leq 0$, a similar calculation yields the result. The same way holds for $H_{v,k}(j\omega)$. ∎

5. Pre-analyses of Phase Contour Lines

As seen in the previous section, both the cross correlation function and the cross spectrum density have complicated forms for the closed loop case. It is difficult to analyze phase contour lines directly. Thus, this section provides preparations for the later analyses. In the section 5. 1, we compare the cross correlation function with the open loop case and consider the outlines of the phase contour plot. Section 5. 2 gives an analysis for individual terms of $\phi_{uy}(\tau)$ and $\Phi_{uy}(\omega)$. Both of them are composed of the terms related to an integer times the dead time of the system. We investigate phase contour lines of each term separately.

5. 1 Difference from Open Loop Case and Outlines of Phase Contour Lines

For open loop systems, if there is no correlation between $u(t)$ and $v(t)$,

$$\phi_{uy}(\tau) = \int_{-\infty}^{+\infty} g_R(\tau - t)\phi_{uu}(t - L)\mathrm{d}t, \qquad (28)$$

where $g_R(t)$ is the impulse response of $G_R(s)$. Let us compare this equation and the equation (17). We will notice

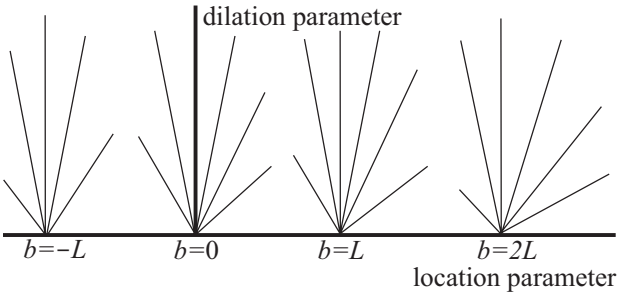

Fig. 3 Phase contour line plots of the closed loop case. The contour lines may concentrate at every $b = kL$ ($k = \cdots, -1, 0, 1, 2, \cdots$) as $a \to 0$.

the following facts.

(1) The closed loop one consists of multiple terms and contains $\phi_{rr}(t - kL)$ and $\phi_{vv}(t - kL)$ for every integer k, whereas the open loop one has only $\phi_{uu}(t - L)$, which corresponds to $k = 1$.

(2) Each integral is a convolution of two functions: auto correlation function shifted along the time axis by kL, which is an integer times of the dead time, and a function that consists of impulse responses of system elements and doesn't contain a dead time term. The form is common to both open and closed loop system.

When the measured system is open loop, the phase contour lines converge at only one point $(0, L)$. For closed loop, however, the former fact implies different behaviors. The contour lines can be drawn into multiple points. Moreover, the contours become complicated due to interactions among the terms. The later indicates that each integral has the same form even if the system is closed loop. If we can extract each term from the equation (17) and calculate its wavelet transform, it could be expected that the phase contours of the wavelet transform concentrate at $b = kL$ (k is integer). From the above observation, for the closed loop systems, we can imagine that the phase contour lines of $\tilde{\phi}_{uy}(a, b)$ gather around multiple points where the location parameter is equal to an integer times of the dead time (**Fig. 3**).

5.2 Phase Contour Analysis for Each Term

For the closed loop case, $\phi_{uy,k}(\tau)$ is the sum of multiple terms related to different time delays. We will analyze phase contour lines for each term. The analysis is a preparation for the next section. Our interest is an analysis of the phase contour lines when a approaches zero. In other words, behaviors in relatively higher frequency bands. Therefore we can assume $|G_{LP}(j\omega)| < 1$ and employ the lemma 6.

At first, we denote the k-th term of the first summation of the equation (26) by $\Phi_{uy,k}(\omega)$, that is

$$\Phi_{uy,k}(\omega) = \boldsymbol{H}_k(j\omega)\boldsymbol{\Phi}_{rr,vv}(\omega)e^{-j\omega kL}. \quad (29)$$

It is possible to relate $\Phi_{uy,k}(\omega)$ with the k-th term in the first summation of the equation (17), that is

$$\phi_{uy,k}(\tau) = \int_{-\infty}^{+\infty} \boldsymbol{h}_k^T(\tau - t)\boldsymbol{\phi}_{rr,vv}(t - kL)\mathrm{d}t. \quad (30)$$

This is due to the stability assumption of the system. In the rest of the paper, we ignore the second line of the equation (26) and assume $\Phi_{uy}(\omega) \approx \sum_{k=-\infty}^{+\infty} \Phi_{uy,k}(\omega)$.

Let $\tilde{\phi}_{uy,k}(a, b)$ be the wavelet transform corresponding to $\Phi_{uy,k}(\omega)$. The result of the section 2.1 gives the following expression.

$$\tilde{\phi}_{uy,k}(a, b) \approx \frac{\psi^*(0)}{\sqrt{a}}\boldsymbol{H}_k\Big(\frac{j\omega_p}{a}\Big)\boldsymbol{\Phi}_{rr,vv}\Big(\frac{\omega_p}{a}\Big)e^{j\omega_p(b-kL)/a}$$

From (27), $\angle \boldsymbol{H}_k(j\omega) = \angle G_R(j\omega) + (k-1)\angle G_{LP}(j\omega)$. Thus $\angle\tilde{\phi}_{uy,k}(a, b) \approx \angle G_R(j\omega_p/a) + (k-1)\angle G_{LP}(j\omega_p/a) - \angle\psi(0) + (b - kL)\omega_p/a$ because $\boldsymbol{\Phi}_{rr}(\omega_p/a)$ is real. Consequently, phase contour lines for $\tilde{\phi}_{uy,k}(a, b)$ can be expressed as

$$b \approx \frac{1}{\omega_p}(\angle G_R(j\omega_p/a) + (k-1)\angle G_{LP}(j\omega_p/a) - \angle\tilde{\phi}_{uy,k}(a, b) - \angle\psi(0))a + kL. \quad (31)$$

This equation shows that the contour lines for integer k converge at $b = kL$ as $a \to 0$ (Fig. 3).

The result does not directly mean that the phase contour lines concentrate at $b = kL$ for each integer k. We plot the phase contours of $\tilde{\phi}_{uy}(a, b)$, that is the sum of $\tilde{\phi}_{uy,k}(a, b)$. Thus $\angle\tilde{\phi}_{uy}(a, b)$ is affected by multiple terms and its behavior is not simple in general. Nevertheless, it implies that $b = kL$ are candidate points where the phase contours gather. It agrees with the expectation in the section 5.1.

Remark: When defining $\Phi_{uy,k}(\omega)$, the second summation of (26) is ignored. We will note a phase value for each term of the summation. In fact, the phase value of $(G_{LP}^*(j\omega))^{-k}G_{C2}^*(j\omega)$ is identical to the one of $\boldsymbol{H}_k(j\omega)$, that is $\angle((G_{LP}^*(j\omega))^{-k}G_{C2}^*(j\omega)) = \angle G_R(j\omega) + (k-1)\angle G_{LP}(j\omega) = \angle\boldsymbol{H}_k(j\omega)$. It can be proven by using $G_{LP}(j\omega) = G_{C2}(j\omega)G_R(j\omega)$. Hence even if the definition of $\Phi_{uy,k}(\omega)$ includes a term in the second summation, there is no effect on phase contour lines related to $e^{-j\omega kL}$. However, the later analyses become too difficult if adding the second summation. Thus we don't discuss any more.

6. Detailed Analyses of Phase Contour Lines

The objective of this section is to analyze the phase contour lines for the closed loop case by using the above

results. In order to complete our analysis, additional assumptions are necessary. Thus we focus two cases with appropriate conditions. The one case is that each term of the equation (17) is localized in time domain, so that interactions between the terms can be ignored. The result of the section 5.2 is available for this case. The other is that the gain of the loop transfer function is suppressed. In fact, the result of the latter is identical to the open loop case because $\tilde{\phi}_{uy,k}(a,b)$ becomes negligible except for $k=1$.

6.1 Case 1: Each Term Is Separated in Time Domain

Recall the assumption $\phi_{uy}(\tau) \approx \sum_{k=-\infty}^{+\infty} \phi_{uy,k}(\tau)$ for simplicity. If the contribution of $\phi_{uy,k}(\tau)$ to $\phi_{uy}(\tau)$ is dominant around $\tau = kL$, $\tilde{\phi}_{uy,k}(a,b)$ is also expected to be dominant and a good approximation of $\tilde{\phi}_{uy}(a,b)$ around $b = kL$. We show below that if $\phi_{rr,vv}(\tau)$, $\boldsymbol{h}_k(\tau)$ and $\psi(t)$ are exponentially decreasing function localized around the origin, then $\tilde{\phi}_{uy,k}(a,b)$ is also exponentially decreasing and localized around $b = kL$. Now, suppose three conditions.

(1) There exist positive constants C_r, C_v, and α_{rv} such that $|\phi_{rr}(\tau)| < C_r e^{-\alpha_{rv}|\tau|}$ and $|\phi_{vv}(\tau)| < C_v e^{-\alpha_{rv}|\tau|}$. Auto correlation functions of usual signals satisfy this condition except for periodic signals.

(2) There exist positive constants C_h and α_h such that $|h_{r,k}(t)| < C_h e^{-\alpha_h|t|}$ and $|h_{v,k}(t)| < C_h e^{-\alpha_h|t|}$. Both $h_{r,k}(t)$ and $h_{v,k}(t)$ are composed of convolution integrals between impulse responses of linear stable systems. Hence they are exponentially decaying functions.

(3) There exist positive constants C_{aw} and α_{aw} such that $|\psi(t)| < C_{aw} e^{-\alpha_{aw}|t|}$. It means the analyzing wavelet $\psi(t)$ is localized around the origin and decays exponentially.

Under the assumptions, we have the following lemma.

Lemma 7. If the above three conditions are satisfied, there is a positive constant $C_{\tilde{\phi}}$ such that

$$|\tilde{\phi}_{uy,k}(a,b)| < C_{\tilde{\phi}} e^{-\beta|b-kL|} \tag{32}$$

where $\beta = \min\{\alpha_{rv}, \alpha_h, \alpha_{aw}/a\}$.

Proof: Consider two exponentially decaying functions. Their convolution is also exponentially decaying and its decay rate is governed by the slower one. ∎

Lemma 7 shows that $\tilde{\phi}_{uy,k}(a,b)$ becomes exponentially smaller as $|b-kL|$ is larger and the decay rate is governed by the slowest time constant. We need to take acount of α_{rv} and α_h (α_{aw}/a is negligible because it grows when $a \to 0$). If the dead time L is long such that $e^{-\alpha_{rv}L}$ and $e^{-\alpha_h L}$ are sufficiently small, $\tilde{\phi}_{uy,k}(a,b)$ is localized around $b = kL$ and almost vanishes at $b \geq (k+1)L$ and $b \leq (k-1)L$. Therefore we can approximate $\tilde{\phi}_{uy}(a,b)$ around $b = kL$ as

$$\tilde{\phi}_{uy}(a,b) \simeq \tilde{\phi}_{uy,k}(a,b). \tag{33}$$

When this approximation is valid for some integers k, as a tends to zero, the phase contour lines of $\tilde{\phi}_{uy}(a,b)$ converge at the one of $b = kL$ such that the approximation holds. That is, the contour lines concentrate around multiple points. Nevertheless, the dead time is measurable from the interval of the points because the interval is L.

As seen above, for the closed loop case, there is a possibilities that the phase contours concentrate not only at $b = L$ but also multiple points satisfying $b = kL$ (k is integer). It also means that the contours may converge at a point where the location parameter is negative. These properties differ from the open loop case.

6.2 Case 2: Open-Loop Transfer Function Has Small Gain

Consider the equation (27). If $|G_{LP}(j\omega)| < 1$, $|\boldsymbol{H}_k(j\omega)|$ takes a maximum at $k = 1$ and decreases as $|k-1|$ is larger. In addition, if $|G_{LP}(j\omega_p/a)| < 1$, we can derive

$$|\tilde{\phi}_{uy,k}(a,b)| = |G_{LP}(j\omega_p/a)|^{|k-1|} |\tilde{\phi}_{uy,1}(a,b)|.$$

Therefore $|\tilde{\phi}_{uy,k}(a,b)| \ll |\tilde{\phi}_{uy,1}(a,b)|$ for a such that $|G_{LP}(j\omega_p/a)|$ is sufficiently small and $\tilde{\phi}_{uy}(a,b)$ can be approximated as

$$\tilde{\phi}_{uy}(a,b) \simeq \tilde{\phi}_{uy,1}(a,b). \tag{34}$$

Consequently, $\tilde{\phi}_{uy,1}(a,b)$ is dominant over all terms.

As seen in the previous section, phase contours of $\tilde{\phi}_{uy,1}(a,b)$ are expressed by

$$b \approx \frac{\angle G_R(j\omega_p/a) - \angle \tilde{\phi}_{uy,1}(a,b) - \angle \psi(0)}{\omega_p} a + L. \tag{35}$$

For the case considered here, the equation also represents the phase contours of $\tilde{\phi}_{uy}(a,b)$. This is equal to the equation (4), which was derived for the open loop case. Hence the contour lines concentrate at $b = L$ as $a \to 0$. It means that the phase contour plots are not affected by whether a target system is open loop or closed loop, if the open-loop transfer function has sufficiently small gain in higher frequencies.

7. Numerical Example

This section gives two numerical simulations to illustrate validity of discussions in the preceding sections. The former example corresponds to the section 6.1 and the latter to 6.2.

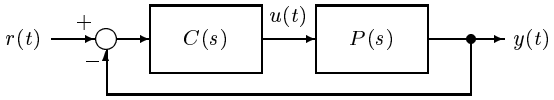

Fig. 4 Configuration of numerical simulations.

Figure 4 shows a configuration of a controller C and a controlled object P in the simulations. Both P and C were SISO LTI systems and only P had a dead time element on its input. We added exogenous inputs $r(t)$ and got $u(t)$ and $y(t)$, which were inputs and outputs of the controlled object respectively. The purpose of the simulation was to measure the dead time of P from the wavelet transform of the cross correlation function between $u(t)$ and $y(t)$.

Example 1: The transfer functions of P and C were

$$P(s) = \frac{5}{s+5}e^{-2s},\ C(s) = 0.98 + \frac{0.1}{s}. \qquad (36)$$

The dead time of P was 2 seconds. The number of samples was set to 8192 and the sampling rate was set to 0.1 second. We generated the input signal $r(t)$ by applying the filter whose transfer function was $1/(5s+1)$ to normally distributed random numbers with variance 1.0. This simulation was carried out under disturbance free. An analyzing wavelet was chosen to be the Gabor function, which is a product of the Gaussian window function and a complex sinusoid, *i.e.* $\psi(t) = \exp(-\omega_p^2 t^2/2\gamma^2)\exp(-j\omega_p t)$. In this simulation, ω_p and γ were set to 1 (rad/sec) and 2π respectively.

Figure 5 is a phase contour plot of $\tilde{\phi}_{uy}(a,b)$. The horizontal axis stands for shift parameter (time) and vertical axis for dilation parameter. Phase contour lines converge at multiple points $b = -4, -2, 0, 2, \cdots$, *i.e.* every two seconds, as a tends to zero. The result shows the validity of the analysis in the section 6. 1.

Example 2: The transfer functions of P and C were

$$P(s) = \frac{1}{s^2+2s+1}e^{-5s},\ C(s) = 0.5 + \frac{0.1}{s}. \qquad (37)$$

The dead time was 5 seconds. We used the same settings as the Example 1 for the number of samples, the sampling rate, the input signal $r(t)$, and the analyzing wavelet.

Figure 6 illustrates a phase contour plot. Solid lines are contours for the closed loop case and dashed lines for open loop. Both contour lines resemble each other and concentrate at $b = 5$, where the dead time is located, as a tends to zero. This agrees with the discussion in the section 6. 2.

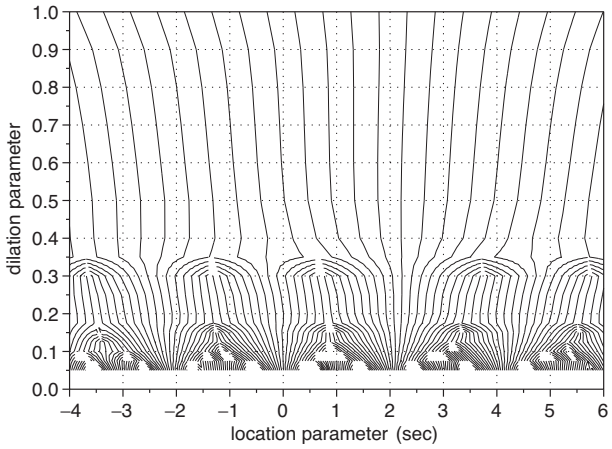

Fig. 5 Phase contour line plots of Example 1.

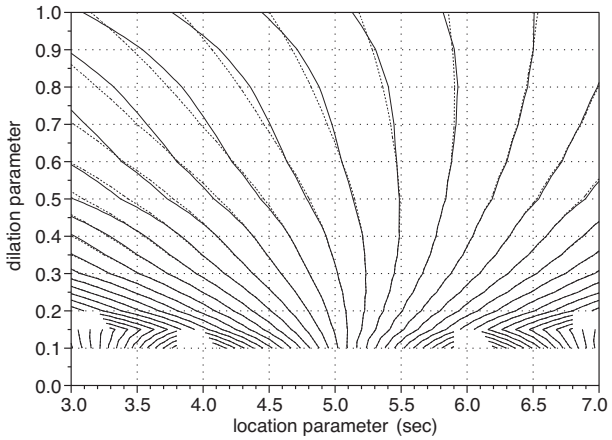

Fig. 6 Phase contour line plots of Example 2.

8. Conclusion

This paper describes that our wavelet based method for dead time measurement is applicable to both open loop systems and stable closed loop systems. We derive a cross correlation function between an input and an output for a measurement target under a closed loop configuration. Our method uses the wavelet transform of the correlation function and its phase contour line plots. We show a possibility that the phase contour lines of the wavelet transform may concentrate at multiple points, which correspond to an integer times the dead time of the system, under certain conditions. Another case is also considered. If the open loop transfer function satisfies a condition on its gain, the phase contour lines behave similarly to the open loop setting. For both cases, our proposed method can measure the dead time. Numerical experiments are carried out to show the validity of the theoretical analyses.

There are some further researches: a theoretical analysis for the case of unstable systems, and evaluation of effects by disturbances.

References

1) Y. Iihoshi, S. Shin, M. Ohta: Detection of Dead Time and Relative Degree using Wavelet Transform, Trans. of IEE Japan, **118-C**-4, 606/610 (1998) (in Japanese)
2) T. Tabaru and S. Shin: Deatd Time Measurement Based on Wavelet Analysis of Correlation Data, Trans. of SICE, **35**-3, 357/362 (1999) (in Japanese)
3) T. Tabaru and S. Shin: "Reconsideration of Dead Time Measurement by Wavelet from Phase Property of Frequency Response", Proceedings of IFAC Symp. SYSID 2000, **2**, 775/779 (2000)
4) T. Tanaru: Wavelet Analysis of Correlation Function and Its Application to Dead Time Measurement, Ph.D. thesis, the University of Tokyo (2003)
5) K. Nakano, T. Tabaru, S. Shin and Y. Toyoda: Identification of Continuous-Time Systems with Time Delay Based on Wavelet Analysis and Its Application to Boiler Process, Trans. of IEE Japan, **119-C**-6, 724/733 (1999) (in Japanese)
6) K. Nakano, T. Tabaru, S. Shin, Y. Toyoda, T. Tsujino and T. Sanematsu: Wavelet-Based Identification for Control of Watertube Drum Boilers, Trans. of IEE Japan, **122-D**-2, 111/119 (2002) (in Japanese)
7) T. Tabaru and S. Shin: Relation between Spectrum Density and Wavelet Transform of Correlation Function, Trans. of SICE, **E-3**, 25/32 (2004)
8) J. Hale (1977): *Theory of Functional Differential Equations*, Springer-Verlag.
9) T. Tabaru and S. Shin: "Dead Time Measurement of Closed Loop System by Wavelet", IFAC Symp. on SYSID 2003, pp. 437-442 (2003)

Tetsuya Tabaru (Member)

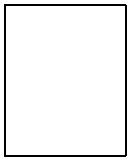

He received the B.E. and M.E. Degrees respectively in 1992 and 1994. He also received Doctor of Engineering from the University of Tokyo in 2003. From 1995 to 2006, he was a Research Associate at the University of Tokyo. Since 2006, he joined Yamatake Corporation.

Shin Seiichi (Member)

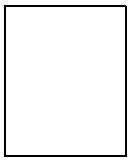

He received B.E. and M.E. Degrees respectively in 1978 and 1980. He also received Doctor of Engineering from the University of Tokyo in 1987. He was awarded Paper Award from the Society of Instrumentation and Control Engineers in 1991, 1992, 1993 and 1998 including the Takeda Prize. He is a Fellow of SICE.